WILEY-VCH

Molecular Design of Naphthalene- and Carbazole-Based Monomers for Regiospecific Synthesis of Poly(arylenevinylene)s via Co-catalyzed Hydroarylation Polyaddition

Ryota Iwamori,[a] Junpei Kuwabara,[a,b] Takeshi Yasuda,[c] Takaki Kanbara*[a]

[a] R. Iwamori, Prof. J. Kuwabara, Prof. T. Kanbara
Institute of Pure and Applied Sciences, University of Tsukuba, 1-1-1 Tennodai, Tsukuba, Ibaraki, 305-8573, Japan.
E-mail: kanbara@ims.tsukuba.ac.jp

[b] Prof. J. Kuwabara
Tsukuba Research Center for Energy Materials Science (TREMS), Institute of Pure and Applied Sciences, University of Tsukuba, 1-1-1 Tennodai, Tsukuba, Ibaraki 305-8573, Japan.

[c] Dr. T. Yasuda
Research Center for Macromolecules and Biomaterials, National Institute for Materials Science (NIMS), 1-2-1 Sengen, Tsukuba, Ibaraki 305-0047, Japan.

Abstract: This study focuses on the development of regiospecific hydroarylation polyaddition of naphthalene- and carbazole-based monomers with diynes under mild reaction conditions at room temperature. A 1-pyrazole substituent serves as an appropriate directing group for a Co-catalyst to efficiently activate the C–H bonds of generally inactive six-membered aromatic hydrocarbons. The 1-pyrazole groups in 2,6-di(1-pyrazolyl)naphthalene adopt planar conformations and act as directing groups, resulting in a smooth hydroarylation reaction. In contrast, the reaction with 1,5-di(1-pyrazolyl)naphthalene did not proceed. The polyaddition reaction of 2,6-di(1-pyrazolyl)naphthalene selectively proceeded at 3,7-positions under mild reaction conditions at 30 °C, and yielded corresponding poly(arylenevinylene) with high molecular weight. This molecular design is also applicable to the hydroarylation polyaddition of carbazole; the polyaddition reaction of 9-(2-ethylhexyl)-3,6-di(1-pyrazolyl)carbazole selectively occurred at 2,7-positions. The optical and electronic properties of the synthesized compounds were evaluated. The obtained poly(arylenevinylene)s served as an emitting material in organic light-emitting diode. This study aims to develop a Co-catalyzed hydroarylation polyaddition via C–H activation of generally inactive polyaromatic hydrocarbons under mild conditions.

Transition-metal-catalyzed C–H functionalization is a powerful approach for C–C bond formation between aromatic compounds without prior preparation of starting materials.[1–5] This approach provides the straightforward synthesis of a vast number of compounds, ranging from small biologically active molecules to macromolecular organic materials.[1,3,6,7] In the research field of polymer chemistry, direct arylation polycondensation,[8–11] cross-dehydrogenative-coupling polycondensation,[9,12–16] and direct alkenylation polycondensation [17–19] have been reported for the synthesis of π-conjugated polymers via C–H activation reactions.

Poly(arylenevinylene)s (PAVs) are promising semiconducting materials used in organic optoelectronic devices such as organic photovoltaics (OPVs), organic field-effect transistors (OFETs), and organic light-emitting diodes (OLEDs).[20–22] PAVs have generally been prepared by polycondensation[23] based on the Gilch reaction,[24,25] Wittig reaction,[26–28] olefin metathesis,[29–32] Migita-Kosugi-Stille cross-coupling,[33] Mizoroki-Heck reaction,[34–36] and transition-metal-mediated dehalogenating polyolefination.[37–39] In recent years, hydroarylation polyaddition of alkynes has been developed to synthesize as an ideal method for the synthesis of PAVs because the production of by-products from monomers can be eliminated. [40–43] We recently reported the Cp*Co(III)-catalyzed hydroarylation polyaddition of aromatic diynes to pyrrole and thiophene derivatives for the preparation of PAVs (Scheme 1a).[41–43] The introduction of appropriate directing groups promoted site- and regio-selective synthesis of the corresponding PAVs under mild reaction conditions even at 30 °C. However, to the best of our knowledge, the C–C bond formation reaction via site-selective C–H bond activation of polyaromatic hydrocarbons (PAHs) at room temperature has not been achieved because the C–H bonds of PAHs are less reactive than those of pyrrole and thiophene.[16,44–46] The cleavage of C–H bonds in PAHs generally requires harsh reaction conditions because of their high activation energies.

To overcome this limitation, we explored the appropriate monomer structures and reaction conditions for the site- and regio-selective hydroarylation polyaddition of PAHs using a Co-catalyst. As poly(naphthalene) and poly(naphthalenevinylene) derivatives linked at β-positions show high fluorescence quantum yields (Φ_{fl} > 0.7) and have been applied to OLEDs,[47,48] 2,6-di(1-pyrazolyl)naphthalene was designed as a new naphthalene monomer. A site- and regio-selective hydroarylation polyaddition proceeded smoothly under mild reaction conditions to obtain the corresponding PAV (Scheme 1b). In addition, this monomer design was applicable to the hydroarylation polyaddition of a carbazole unit. Furthermore, the optical and electronic properties of the synthesized PAVs were evaluated.

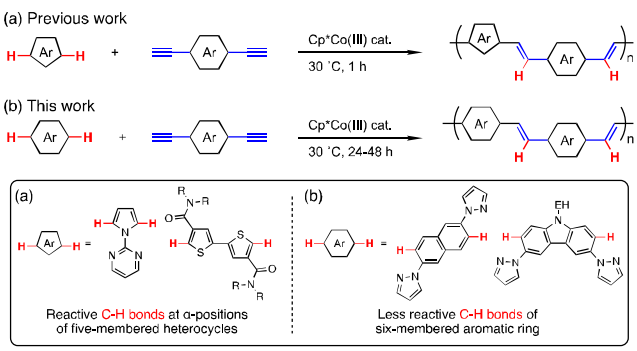

Scheme 1. Cp*Co(III)-catalyzed hydroarylation polyaddition.

In the Cp*Co(III)-catalyzed hydroarylation reaction, the structure of the directing group is a crucial factor that affects the reactivity of the C–H activation step.[49–51] Therefore, to find an appropriate directing group for the Co-catalyzed hydroarylation of less reactive six-membered aromatic compounds, small-molecular model reactions of mono-substituted benzenes (**1**) with 4-ethynyltoluene (**2a**) were tested. Commonly used pyridine-type nitrogens and carbonyl-type oxygens were explored to improve the conversion of benzenes to alkenylated products (Figure 1, and Figures S1–S5). We first attempted the model reaction of 2-phenylpyridine (**1a**) with 2.1 equivalent of **2a** in the presence of $[Cp^*Co(CH_3CN)_3](SbF_6)_2$ (5 mol%) and neodecanoic acid (NDA, 60 mol%) in tetrahydrofuran (THF, 0.1 M) at 30 °C for 24 h under N_2 atmosphere. The product yields of the reaction mixtures were calculated from the nuclear magnetic resonance (NMR) spectra. The reaction afforded the mono-alkenylated product (**3aa**) in 30% yield (Figure S1). The conversion of benzene to alkenylated products improved in the model reaction of 1-phenylpyrazole (**1b**) with **2a**. The NMR yields of the mono-alkenylated product (**3ba**) and di-alkenylated product (**4ba**) were 62% and 18%, respectively (Figure S2). In contrast, carbonyl-type directing groups did not work under these reaction conditions (Figures S3–S5). As a result, the 1-pyrazole substituent was found to be the appropriate directing group for the Co-catalyzed hydroarylation of the benzene moiety. The reaction conditions for **1b** with **2a** were subsequently optimized for efficient hydroarylation (Table S1, Figure S6). A low concentration of the substrate (0.05 M) and the addition of neodecanoic acid (1 equiv.) effectively improved the conversion of **1b** to **3ba** and **4ba**.

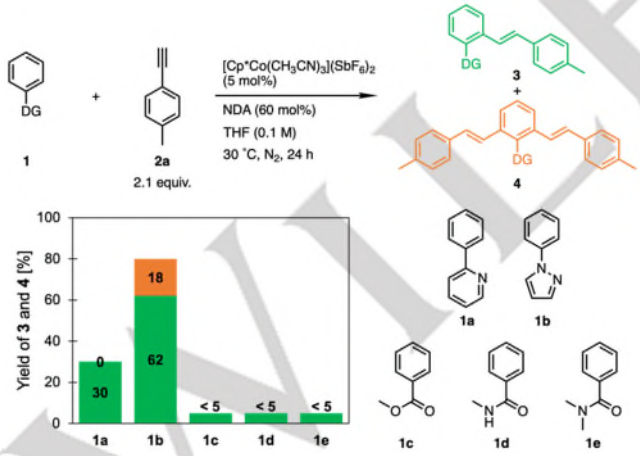

Figure 1. Exploration of the directing group for the benzene moiety. Yields of **3** and **4** were calculated by ^{1}H NMR analyses using 1,3,5-trimethoxybenzene as an internal standard (Figures S1-S5).

Subsequently, 2,6-di(1-pyrazolyl)naphthalene (**5a**) and 1,5-di(1-pyrazolyl)naphthalene (**5b**) were designed for site-selective hydroarylation reaction of naphthalene at β-positions. Small-molecular model reactions of **5a** and **5b** with 4-*tert*-butylphenylacetylene (**2b**) were attempted under the optimized conditions (Scheme 2). The hydroarylation of **5a** selectively proceeded at the 3,7-positions of the naphthalene moiety even at 30 °C, and the dialkenylated product (**6ab**) was isolated in 82% yield (Scheme 2a, Figures S7–S10). In contrast, the hydroarylation of **5b** did not afford the corresponding dialkenylated compound (Scheme 2b, Figure S11). To elucidate the mechanism of the site selectivity and reactivity of **5a** and **5b**, deuterium exchange experiments were performed in the presence of CD_3COOD instead of **2b** and NDA. The selective deuteration of **5a** was observed at the less-hindered 3,7-positions (32% D at the 3,7-positions vs. 0% D at the 1,5-positions; Scheme 3a and Figure S12). Because the Cp*Co(III) catalyst avoids steric repulsion between the Cp* ligand and the C–H bonds at 4,8-positions,[52] the excellent site-selectivity was exhibited at the 3,7-positions (Scheme S1). In contrast, deuterium exchange in **5b** rarely occurred at any position (<5% D, Scheme 3b, and Figure S13). These results indicate that the 1-pyrazole groups introduced at 2,6-positions of naphthalene are suitable for Co-catalyzed hydroarylation. In addition, the molecular geometries were optimized via density functional theory (DFT) calculations using Gaussian at the B3LYP/6-31G(d) level (Figures 2 and S29). Although the 1-pyrazole group of **5a** adopts planar conformations, that of **5b** has difficulty forming planar conformations because of the steric hindrance of the C–H bond at the peri-position. The crystal structures of **5a** and **5b** were ascertained by X-ray crystallography (Table S2 and Figure S30). The dihedral angles between the naphthalene cores and the 1-pyrazole groups in **5a** and **5b**, respectively, were almost consistent with the structures optimized by DFT calculations. These results indicate that the 1-pyrazole group, which easily adopts a planar conformation, acts as an effective directing group for six-membered aromatic hydrocarbons.

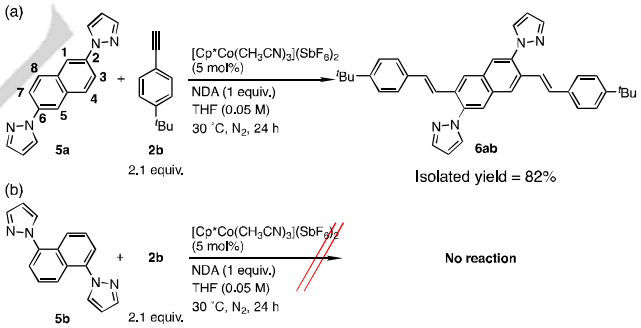

Scheme 2. Hydroarylation reactions of the naphthalene monomers with **2b**.

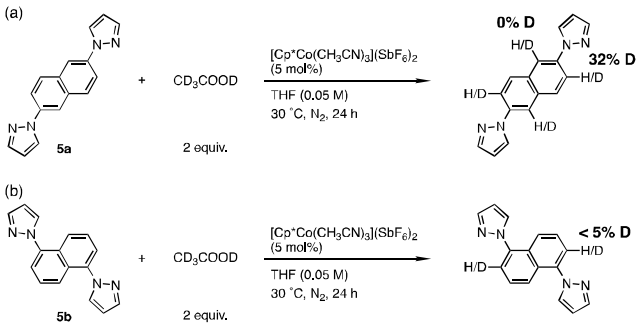

Scheme 3. Deuterium exchange experiments of the naphthalene monomers.

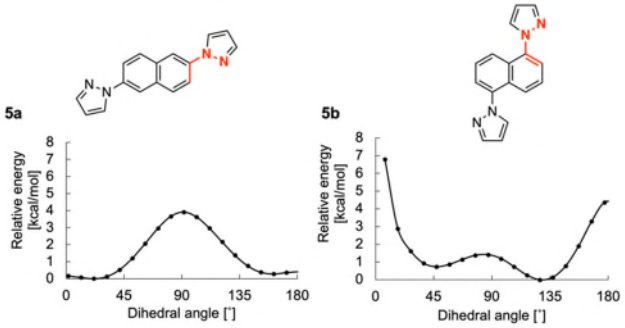

Figure 2. Rotation energies of the 1-pyrazole group of **5a** and **5b**. DFT calculations were carried out at B3LYP/6-31G(d) level.

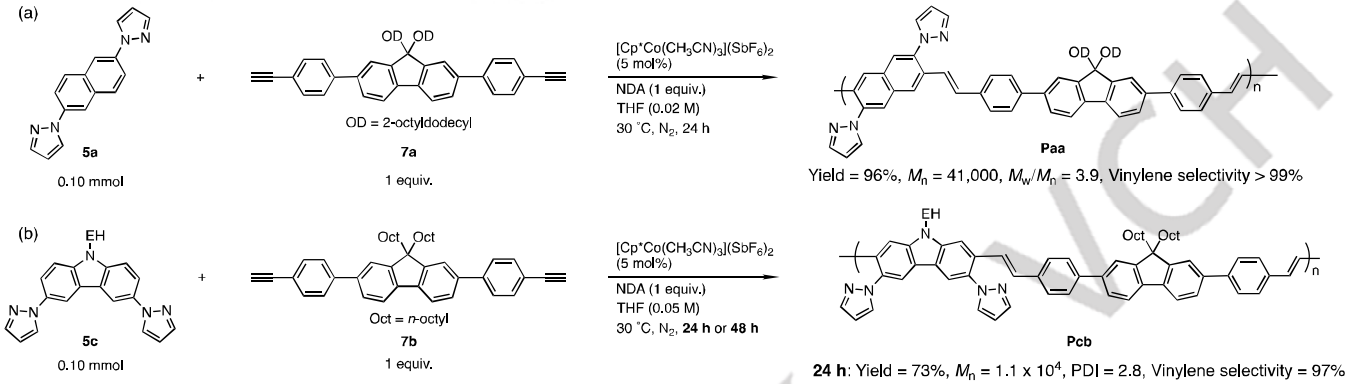

Scheme 4. Hydroarylation polyaddition of the (a) naphthalene- and (b) carbazole-based monomers with diyne monomers.

The hydroarylation polyaddition of **5a** with 2,7-bis(4-ethynylphenyl)-9,9-bis(2-octyldodecyl)fluorene (**7a**) was performed under the same catalytic conditions as the small-molecular model reaction (Scheme 4a). The polyaddition reaction proceeded smoothly even at 30 °C and a low monomer concentration of 0.02 M. The corresponding PAV (**Paa**) was yielded in 96% yield with a number average molecular weight (M_n) of 41,000 and a polydispersity index (M_w/M_n) of 3.9. All signals in the ^{1}H NMR spectrum of **Paa** were assigned to a repeating structure with a 1,2-vinylene unit and terminal structures (Figure 3). No signal assignable to the 1,1-vinylidene unit was observed in the ^{1}H NMR spectrum (5.5–5.0 ppm). Matrix-assisted laser desorption ionization time-of-flight mass spectroscopy (MALDI-TOF-MS) confirmed the structure of the repeating and terminal units derived from each monomer (Figure S14). These results indicate that the hydroarylation of **5a** with **7a** proceeded with quantitative site- and regio-selectivity.

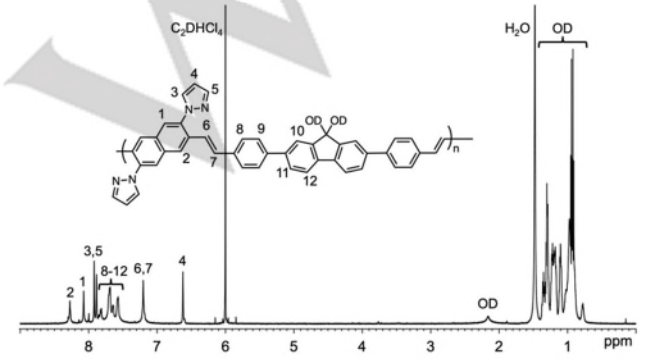

Figure 3. ^{1}H NMR spectrum of **Paa** (600 MHz, $C_2D_2Cl_4$, 373 K).

The same molecular design is compatible with a C–H monomer consisting of a carbazole unit with 1-pyrazole directing groups at the 3,6-positions (Scheme S2 and Figures S15–S17). The hydroarylation polyaddition of 9-(2-ethylhexyl)-3,6-di(1-pyrazolyl)carbazole (**5c**) with 2,7-bis(4-ethynylphenyl)-9,9-di(*n*-octyl)fluorene (**7b**) also gave the corresponding PAV (**Pcb**) in 73% yield with an M_n of 11,000 and an M_w/M_n of 2.8 (Scheme 4b). Moreover, the longer reaction time of the polyaddition reactions increased the molecular weight of **Pcb**; the polyaddition reaction for 48 h gave **Pcb** in 71% yield with an M_n of 23,000 and an M_w/M_n of 3.4. Structural analyses of the synthesized PAVs were conducted by NMR and MALDI-TOF-MS (Figures S18–S20). Almost all the signals in the ^{1}H NMR and MALDI-TOF-MS spectra were assigned to each repeating and terminal structure of the 1,2-vinylene unit, and 3–4% of the 1,1-vinylidene unit was detected in the ^{1}H NMR spectrum (Figures S18 and S19). Formation of the 1,1-vinylidene structure was suppressed by changing the diyne monomer to less steric hindered 4,4'-diethynylbiphenyl (**7c**); the polyaddition reaction of **5c** with **7c** proceeded over 99% of 1,2-vinylene selectivity in 75% yield (Scheme S3, Figures S21 and S22). The molecular weight of **Pcc** could not be measured because **Pcc** was insoluble in THF.

The optical properties of the synthesized monomers, model products, and PAVs were investigated (Table 1). First, we compared a series of naphthalene derivatives in $CHCl_3$ solutions (**5a**, **6ab**, and **Paa**). The ultraviolet-visible (UV-vis) absorption and photoluminescence (PL) spectra are shown in Figure 4. All three molecules showed an absorption band at approximately 300 nm due to π-π* transition of the 2,6-di(1-pyrazolyl)naphthalene core. The model product (**6ab**) had two absorption peaks at 302 and 361 nm. The longer-wavelength absorption at 361 nm was attributed to the conjugated main chain of 3,7-naphthalenevinylene. The absorption maxima of **Paa** was red-shifted compared with those of **5a** and **6ab**, which was caused by the π-extension. The PL spectra exhibited trends

similar to those observed in the absorption spectra. The emission peaks of **5a**, **6ab**, and **Paa** were observed at 358, 425, and 460 nm, respectively. The intensities of the emission peaks of **6ab** and **Paa** were much higher than those of **5a**, which is due to the rigid backbone of 3,7-naphthalenevinylene. The photoluminescence quantum yields (PLQY) of **6ab** and **Paa** in $CHCl_3$ solutions were estimated to be 84 and 80%, respectively. While the PLQY of the carbazole-based PAV (**Pcb**) in $CHCl_3$ solutions was slightly lower than that of the naphthalene-based PAV (**Paa**); the optical spectra of **Paa** and **Pcb** are almost consistent (Figure S31). In addition, the 1-pyrazole substituent did not affect the absorption and PL properties, as supported by the optical spectra and PLQY of the naphthalene- and carbazole-based model compounds without 1-pyrazole groups (**8a** and **8b**; Table S3 and Figure S32). The UV-vis absorption and PL spectra in the film state were also evaluated (Table S3, Figures S33 and S34). While the absorption spectra were consistent with those in $CHCl_3$ solutions, the PL spectra were red-shifted due to the intermolecular π-π stacking in the film states. The PLQY values in the film state decreased because of aggregation-caused quenching (ACQ),[53,54] whereas **Paa** had emission properties as high as those of PAV for OLEDs.[55] Atomic force microscopy (AFM) and X-ray diffraction (XRD) analyses revealed that the spin-coated films of **Paa** and **Pcb** were amorphous (Figure S35).

Table 1. Optical properties of the monomer, model compounds, and PAVs. [a]

Compound	λ_{abs} [nm]	λ_{em} [nm]	PLQY [%] [b]
5a	267, 308	358	-
6ab	302, 361	425	84
Paa	405	460	80
Pcb	406	454	66

[a] Optical properties were measured in $CHCl_3$ solution at concentrations of 5.0 x 10^{-6} M. [b] Photoluminescence quantum yield.

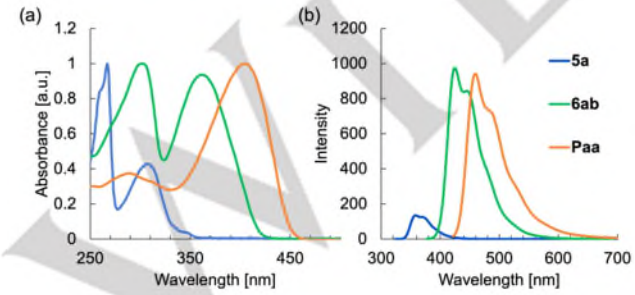

Figure 4. Optical spectra of the naphthalene derivatives (monomer: **5a**, model product: **6ab**, and PAV: **Paa**) in $CHCl_3$ solutions (5.0 x 10^{-6} M). (a) UV-vis absorption spectra. (b) PL spectra.

Because the **Paa** film exhibited light-green emissions (λ_{em} = 472 and 494 nm, quantum yield (φ) = 20%) when excited at 400 nm, the electroluminescent (EL) properties of **Paa** were evaluated in OLED (Figure 5, see the Supporting Information for the details of OLED fabrication). The EL spectrum was slightly red-shifted from the PL spectrum because of the interference effect between the emitted light that directly traveled from the emissive layer to the ITO electrode and the light that was reflected once from the Al electrode.[56] The coordinates of the CIE chromaticity diagram were x = 0.285 and y = 0.451 at 1.43 mA cm^{-2} (Figure S36). The luminance reached 323 cd m^{-2} at a current density of 80.4 mA cm^{-2}, and the external quantum efficiency (EQE) of the OLED was 0.32% at 4.6 mA cm^{-2} (Figure S37). These results indicate that **Paa** serves as an emitting material for OLEDs.

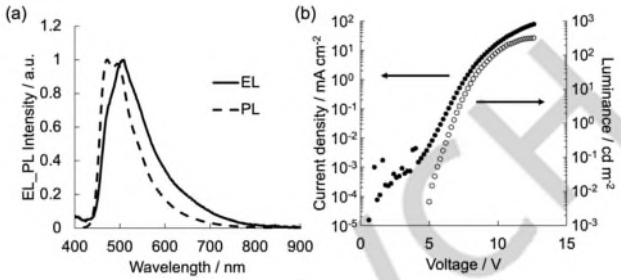

Figure 5. (a) PL spectrum of the thin film of **Paa** and EL spectrum of the OLED using **Paa** and (b) Current density-voltage-luminance characteristics for the fabricated OLED.

In summary, naphthalene- and carbazole-based monomers were designed via Co-catalyzed hydroarylation polyaddition under mild conditions for the regiospecific synthesis of poly(arylenevinylene)s. The 1-pyrazole substituent was suitable as the directing group for the C–H activation of six-membered aromatic rings. The introduction of the 1-pyrazole substituent at the 2,6-positions of the naphthalene moiety was effective in selectively activating the C–H bonds at the 3,7-positions owing to the planar conformations of the 1-pyrazole substituents. The molecular design of the aromatic monomer was versatile, not only for the naphthalene unit but also for the carbazole unit. The hydroarylation polyaddition of the designed naphthalene- and carbazole-based monomers proceeded under mild conditions at room temperature without producing by-products. Notably, hydroarylation polyaddition expands the C–H functionalization strategies for the synthesis of PAVs to generally inactive PAH monomers. The synthesized PAVs showed a high PLQY and served as emitting layers in OLEDs. Further molecular designs for the synthesis of high-performance PAVs are currently underway.

Acknowledgements

The authors thank the Chemical Analysis Division and the OPEN FACILITY, Research Facility Center for Science and Technology, University of Tsukuba for the measurements of NMR, X-ray crystallographic analyses, and MALDI-TOF-MS. This work was partly supported by JSPS KAKENHI Grant Numbers 23K04835 and 23KJ0240.

Conflict of interest

The authors declare no conflict of interest.

Keywords: Cobalt • Hydroarylation • π-Conjugated polymer • Polyaromatic hydrocarbon • Organic light-emitting diode

[1] J. Yamaguchi, A. D. Yamaguchi, K. Itami, *Angew. Chem. Int. Ed.* **2012**, *51*, 8960–9009.
[2] P. B. Arockiam, C. Bruneau, P. H. Dixneuf, *Chem. Rev.* **2012**, *112*, 5879–5918.
[3] J. Wencel-Delord, F. Glorius, *Nat. Chem.* **2013**, *5*, 369–375.
[4] T. Gensch, M. N. Hopkinson, F. Glorius, J. Wencel-Delord, *Chem. Soc. Rev.* **2016**, *45*, 2900–2936.
[5] J. R. Hummel, J. A. Boerth, J. A. Ellman, *Chem. Rev.* **2017**, *117*, 9163–9227.
[6] L. Xing, C. K. Luscombe, *J. Mater. Chem. C* **2021**, *9*, 16391–16409.
[7] J. Kuwabara, T. Kanbara, *ChemPlusChem* **2024**, *89*, e202300400.
[8] L. G. Mercier, M. Leclerc, *Acc. Chem. Res.* **2013**, *46*, 1597–1605.
[9] J. Kuwabara, T. Kanbara, *Macromol. Rapid Commun.* **2021**, *42*, 2000493.
[10] L. Ye, B. C. Thompson, *J. Polym. Sci.* **2022**, *60*, 393–428.
[11] B. Z. Yongrui He, Lijun Huo, *Nano Energy* **2024**, *123*, 109397.
[12] H. Aoki, H. Saito, Y. Shimoyama, J. Kuwabara, T. Yasuda, T. Kanbara, *ACS Macro Lett.* **2018**, *7*, 90–94.
[13] C. Tanaka, J. Kuwabara, T. Yasuda, T. Kanbara, *Synth. Met.* **2019**, *254*, 180–183.
[14] N. Onda, R. Sato, J. Kuwabara, T. Yasuda, T. Kanbara, *Synth. Met.* **2023**, *293*, 117279.
[15] B. Chakraborty, C. K. Luscombe, *Angew. Chem. Int. Ed.* **2023**, *62*, e202301247.
[16] G. Albano, *Org. Chem. Front.* **2024**, *11*, 1495–1622.
[17] H. Saito, J. Kuwabara, T. Yasuda, T. Kanbara, *Polym. Chem.* **2016**, *7*, 2775–2779.
[18] H. Saito, J. Kuwabara, T. Yasuda, T. Kanbara, *Macromol. Rapid Commun.* **2018**, *39*, 1800414.
[19] J. Lee, H. J. Park, J. M. Joo, D.-H. Hwang, *Macromol. Res.* **2019**, *27*, 115–118.
[20] A. Kraft, A. C. Grimsdale, A. B. Holmes, *Angew. Chem. Int. Ed.* **1998**, *37*, 402–428.
[21] Y. Wang, T. Hasegawa, H. Matsumoto, T. Michinobu, *J. Am. Chem. Soc.* **2019**, *141*, 3566–3575.
[22] C. Yang, S. Zhang, J. Hou, *Aggregate* **2022**, *3*, e111.
[23] A. J. Blayney, I. F. Perepichka, F. Wudl, D. F. Perepichka, *Isr. J. Chem.* **2014**, *54*, 674–688.
[24] H. G. Gilch, W. L. Wheelwright, *J. Polym. Sci. Part A-1 Polym. Chem.* **1966**, *4*, 1337–1349.
[25] H. Becker, H. Spreitzer, K. Ibrom, W. Kreuder, *Macromolecules* **1999**, *32*, 4925–4932.
[26] R. N. McDonald, T. W. Campbell, *J. Am. Chem. Soc.* **1960**, *82*, 4669–4671.
[27] S. Pfeiffer, H. H. Hörhold, *Synth. Met.* **1999**, *101*, 109–110.
[28] D. A. M. Egbe, H. Neugebauer, N. S. Sariciftci, *J. Mater. Chem.* **2011**, *21*, 1338–1349.
[29] H. Weychardt, H. Plenio, *Organometallics* **2008**, *27*, 1479–1485.
[30] T. Haque, K. Nomura, *Catalysts* **2015**, *5*, 500–517.
[31] V. P. Conticello, D. L. Gin, R. H. Grubbs, *J. Am. Chem. Soc.* **1992**, *114*, 9708–9710.
[32] S. W. Chang, M. Horie, *Chem. Commun.* **2015**, *51*, 9113–9116.
[33] J. Dhar, T. Mukhopadhay, N. Yaacobi-Gross, T. D. Anthopoulos, U. Salzner, S. Swaraj, S. Patil, *J. Phys. Chem. B* **2015**, *119*, 11307–11316.
[34] H. N. Cho, J. K. Kim, D. Y. Kim, C. Y. Kim, N. W. Song, D. Kim, *Macromolecules* **1999**, *32*, 1476–1481.
[35] J. Pei, S. Wen, Y. Zhou, Q. Dong, Z. Liu, J. Zhang, W. Tian, *New J. Chem.* **2011**, *35*, 385–393.
[36] T. Zhang, J. Wang, M. Zhou, L. Ma, G. Yin, G. Chen, Q. Li, *Tetrahedron* **2014**, *70*, 2478–2486.
[37] H.-H. Horhold, J. Gottschaldt, J. Opferman, *J. Prakt. Chem.* **1977**, *319*, 611–621.
[38] S. Baysec, E. Preis, S. Allard, U. Scherf, *Macromol. Rapid Commun.* **2016**, *37*, 1802–1806.
[39] P. Klein, H. J. Jötten, C. M. Aitchison, R. Clowes, E. Preis, A. I. Cooper, R. S. Sprick, U. Scherf, *Polym. Chem.* **2019**, *10*, 5200–5205.
[40] S. Selmani, L. Vanderzwet, A. J. Kukor, D. J. Schipper, *Synlett* **2018**, *29*, 2552–2556.
[41] R. Iwamori, R. Sato, J. Kuwabara, T. Yasuda, T. Kanbara, *Macromol. Rapid Commun.* **2021**, *42*, 2100283.
[42] R. Iwamori, R. Sato, J. Kuwabara, T. Kanbara, *Polym. Chem.* **2022**, *13*, 379–382.
[43] R. Iwamori, J. Kuwabara, T. Yasuda, T. Kanbara, *Macromolecules* **2023**, *56*, 5407–5414.
[44] D. Lapointe, K. Fagnou, *Chem. Lett.* **2010**, *39*, 1118–1126.
[45] L. Xing, J. R. Liu, X. Hong, K. N. Houk, C. K. Luscombe, *J. Am. Chem. Soc.* **2022**, *144*, 2311–2322.
[46] R. Sato, T. Iida, T. Kanbara, J. Kuwabara, *Chem. Commun.* **2022**, *58*, 11511–11514.
[47] T. Mori, M. Kijima, *Eur. Polym. J.* **2009**, *45*, 1149–1157.
[48] V. Sannasi, P. Manikandan, B. G. Sundararaj, M. T. Vijayan, D. Jeyakumar, *Iran. Polym. J.* **2010**, *19*, 969–981.
[49] D. Wei, X. Zhu, J. L. Niu, M. P. Song, *ChemCatChem* **2016**, *8*, 1242–1263.
[50] M. Moselage, J. Li, L. Ackermann, *ACS Catal.* **2016**, *6*, 498–525.
[51] T. Yoshino, S. Matsunaga, *Adv. Synth. Catal.* **2017**, *359*, 1245–1262.
[52] B. Sun, T. Yoshino, M. Kanai, S. Matsunaga, *Angew. Chem. Int. Ed.* **2015**, *54*, 12968–12972.
[53] X. Ma, R. Sun, J. Cheng, J. Liu, F. Gou, H. Xiang, X. Zhou, *J. Chem. Educ.* **2016**, *93*, 345–350.
[54] J.-H. Hsu, W. Fann, P.-H. Tsao, K.-R. Chuang, S.-A. Chen, *J. Phys. Chem. A* **1999**, *103*, 2375–2380.
[55] E. W. Snedden, L. A. Cury, K. N. Bourdakos, A. P. Monkman, *Chem. Phys. Lett.* **2010**, *490*, 76–79.
[56] T. Tsutsui, K. Yamamato, *Jpn. J. Appl. Phys.* **1999**, *38*, 2799–2803.

Entry for the Table of Contents

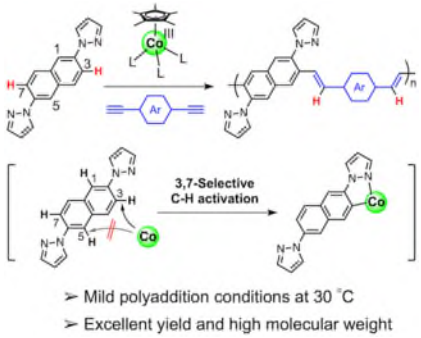

The 1-pyrazole groups in 2,6-di(1-pyrazolyl)naphthalene adopt planar conformations and act as appropriate directing groups for generally inactive six-membered aromatic hydrocarbons, resulting in smooth hydroarylation reaction. The polyaddition reaction of 2,6-di(1-pyrazolyl)naphthalene selectively proceeds at 3,7-positions under mild reaction conditions of 30 °C, and yields corresponding poly(arylenevinylene) with high molecular weight.

WILEY-VCH